Anal. Chem. **2010,** *82,* 8711–8716

Low-Potential Photoelectrochemical Biosensing Using Porphyrin-Functionalized TiO_2 Nanoparticles

Wenwen Tu, Yitong Dong, Jianping Lei,* and Huangxian Ju*

Key Laboratory of Analytical Chemistry for Life Science (Ministry of Education of China), Department of Chemistry, Nanjing University, Nanjing 210093, P. R. China

A novel photoelectrochemical biosensing platform for the detection of biomolecules at relatively low applied potentials was constructed using porphyrin-functionalized TiO_2 nanoparticles. The functional TiO_2 nanoparticles were prepared by dentate binding of TiO_2 with sulfonic groups of water-soluble [meso-tetrakis(4-sulfonatophenyl)porphyrin] iron(III) monochloride (FeTPPS) and characterized by transmission electron microscopy; contact angle measurement; and Raman, X-ray photoelectron, and ultraviolet−visible absorption spectroscopies. The functional nanoparticles showed good dispersion in water and on indium tin oxide (ITO) surface. The resulting FeTPPS-TiO_2-modified ITO electrode showed a photocurrent response at +0.2 V to a light excitation at 380 nm, which could be further sensitized through an oxidation process of biomolecules by the hole-injected FeTPPS. Using glutathione as a model, a methodology for sensitive photoelectrochemical biosensing at low potential was thus developed. Under optimal conditions, the proposed photoelectrochemical method could detect glutathione ranging from 0.05 to 2.4 mmol L^{-1} with a detection limit of 0.03 mmol L^{-1} at a signal-to-noise ratio of 3. The photoelectrochemical biosensor had an excellent specificity against anticancer drugs and could be successfully applied to the detection of reduced glutathione in gluthion injection, showing a promising application in photoelectrochemical biosensing.

Photoelectrochemical measurement is a newly developed technique for the detection of biomolecules.[1,2] Coupling photoirradiation with electrochemical detection, photoelectrochemical sensors have the advantages of both optical methods and electrochemical sensors.[3,4] Thus, this technique shows promising analytical applications and has attracted considerable interest. Some metal oxide semiconductor nanoparticles such as ZnO, ZrO_2, and TiO_2 have been used as significant photoelectrochemical materials. Among them, TiO_2 nanoparticles have been extensively investigated for various photoelectrochemical applications because of their wide band gap, high photoelectrochemical activity under UV irradiation, and strong oxidizing power when illuminated.[1] The photoelectrochemical response from illuminated TiO_2 has been used for the design of photoelectrochemical sensors.[5,6] The integration of Au-doped TiO_2 nanotubes with acetylcholinesterase has led to a rapid and valid photoelectrochemical approach for the determination of acetylcholinesterase inhibition with illumination at 253.7 nm.[7] A dopamine-coordinated photoactive TiO_2 nanoporous film has also been used successfully for the sensitive detection of dihydronicotinamide adenine dinucleotide.[8] Recently, porphyrins, an important class of conjugated organic molecules for light harvesting,[9−11] have been widely used for improving the photo-current conversion efficiency of TiO_2 nanoparticles in molecular electronics and photoelectrochemical devices, especially for solar cells.[12−20] However, the improved photoelectrochemical efficiency has not yet been applied to the construction of a photoelectrochemical biosensing platform.

Porphyrin molecules exhibit ultrafast electron injection, slow charge-recombination kinetics, high absorption coefficients, and

* Corresponding authors. Phone and Fax: +86-25-83593593. E-mail: hxju@nju.edu.cn (H.J.), jpl@nju.edu.cn.

(1) Wang, G.-L.; Xu, J.-J.; Chen, H.-Y.; Fu, S.-Z. *Biosens. Bioelectron.* **2009**, *25*, 791–796.
(2) Wang, G.-L.; Yu, P.-P.; Xu, J.-J.; Chen, H.-Y. *J. Phys. Chem. C* **2009**, *113*, 11142–11148.
(3) Haddour, N.; Chauvin, J.; Gondran, C.; Cosnier, S. *J. Am. Chem. Soc.* **2006**, *128*, 9693–9698.
(4) Ikeda, A.; Nakasu, M.; Ogasawara, S.; Nakanishi, H.; Nakamura, M.; Kikuchi, J. *Org. Lett.* **2009**, *11*, 1163–1166.
(5) Zhao, H. J.; Jiang, D. L.; Zhang, S. Q.; Catterall, K.; John, R. *Anal. Chem.* **2004**, *76*, 155–160.
(6) Zhou, H.; Gan, X.; Wang, J.; Zhu, X. L.; Li, G. X. *Anal. Chem.* **2005**, *77*, 6102–6104.
(7) Zhu, W.; An, Y.-R.; Luo, X.-M.; Wang, F.; Zheng, J.-H.; Tang, L.-L.; Wang, Q.-J.; Zhang, Z.-H.; Zhang, W.; Jin., L.-T. *Chem. Commun.* **2009**, 2682–2684.
(8) Wang, G.-L.; Xu, J.-J.; Chen, H.-Y. *Biosens. Bioelectron.* **2009**, *24*, 2494–2498.
(9) Sgobba, V.; Guldi, D. M. *Chem. Soc. Rev.* **2009**, *38*, 165–184.
(10) Baskaran, D.; Mays, J. W.; Zhang, X. P.; Bratcher, M. S. *J. Am. Chem. Soc.* **2005**, *127*, 6916–6917.
(11) Guldi, D. M.; Rahman, G. M. A.; Zerbetto, F.; Prato, M. *Acc. Chem. Res.* **2005**, *38*, 871–878.
(12) Rochford, J.; Chu, D.; Hagfeldt, A.; Galoppini, E. *J. Am. Chem. Soc.* **2007**, *129*, 4655–4665.
(13) Mozer, A. J.; Wagner, P.; Officer, D. L.; Wallace, G. G.; Campbell, W. M.; Miyashita, M.; Sunahara, K.; Mori, S. *Chem. Commun.* **2008**, 4741–4743.
(14) Tanaka, M.; Hayashi, S.; Eu, S.; Umeyama, T.; Matano, Y.; Imahori, H. *Chem. Commun.* **2007**, 2069–2071.
(15) Kathiravan, A.; Kumar, P. S.; Renganathan, R.; Anandan, S. *Colloids Surf. A: Physicochem. Eng. Aspects* **2009**, *333*, 175–181.
(16) Eu, S.; Hayashi, S.; Umeyama, T.; Oguro, A.; Kawasaki, M.; Kadota, N.; Matano, Y.; Imahori, H. *J. Phys. Chem. C* **2007**, *111*, 3528–3537.
(17) Ikeda, A.; Tsuchiya, Y.; Konishi, T.; Ogasawara, S.; Kikuchi, J. *Chem. Mater.* **2005**, *17*, 4018–4022.
(18) Hayashi, S.; Tanaka, M.; Hayashi, H.; Eu, S.; Umeyama, T.; Matano, Y.; Araki, Y.; Imahori, H. *J. Phys. Chem. C* **2008**, *112*, 15576–15585.
(19) Rochford, J.; Galoppini, E. *Langmuir* **2008**, *24*, 5366–5374.
(20) Yu, J. H.; Chen, J. R.; Wang, X. S.; Zhang, B. W.; Cao, Y. *Chem. Commun.* **2003**, 1856–1857.

10.1021/ac102070f
Published on Web 09/21/2010

good chemical stability. The carboxylic or sulfonic groups on some porphyrins can spontaneously bind to TiO_2 nanoparticles by bridging ester-like or bidentate interactions.[12−16,18,21] The resulting hybrid of porphyrin−TiO_2 nanoparticles shows reduced electron lifetime and, consequently, lower photoinduced electron density under illumination compared to commonly used ruthenium-dye- (N719-) sensitized solar cells,[13] and they can improve by a factor of 2 the power conversion efficiency of dye-sensitized TiO_2 solar cells.[14] The photoelectrochemical behavior of para- and meta-substitued porphyrin sensitizers suggests that both the binding geometry and the distance of the sensitizer from the metal oxide surface dramatically influence the sensitizing effciency.[12] A porphyrinatozinc(II)-(Zn5S-) sensitized TiO_2 solar cell can produce a maximum incident photocurrent efficiency of 65% and a maximum power conversion efficiency of 3.1%.[16] Furthermore, a strong electronic coupling between porphyrin and the TiO_2 surface in porphyrin-sensitized cells has been observed because of the efficient electron injection from the porphyrin excited single state to the conduction band of the illuminated TiO_2.[18] Based on these advantages of porphyrin-functionalized TiO_2 nanoparticles in photoelectrochemistry, this work involved the synthesis of novel functional TiO_2 nanoparticles using water-soluble [meso-tetrakis(4-sulfonatophenyl) porphyrin] iron(III) monochloride (FeTPPS) through the dentate binding of TiO_2 nanoparticles with sulfonic groups of FeTPPS. The nanoparticles showed a stable photoelectrochemical response that could be further sensitized through an electron-transfer process from biomolecule to porphyrin and then to the illuminated TiO_2, leading to a novel application of porphyrin-functionalized TiO_2 nanoparticles as a photoelectrochemical biosensing platform. Using glutathione (GSH) as a model, a novel method for the detection of GSH was thus developed.

GSH, as the most abundant cellular thiol, plays an important role in many biological functions involving antioxidant defense, signal transduction, and cell proliferation.[22] Its level is directly related to many diseases such as cancers, AIDs, neurodegenerative disease, and Alzheimer's and Parkinson's diseases.[23−25] Therefore, the monitoring of GSH in physiological media has gained considerable attention. Several strategies, including microchip electrophoresis-laser induced fluorescence,[26] electrogenerated chemiluminescence of quantum dots,[27] absorption[28] and fluorescent spectroscopies,[29−33] surface-enhanced Raman scattering,[34] and laser desorption/ionization mass spectrometry,[35] have been proposed for this purpose. Several electrochemical methods have also been developed for in situ or online monitoring of GSH.[36−39] However, the high overpotential for the oxidation of GSH limits the application of these electrochemical methods.[38,39] In this work, the photoelectrochemical response of FeTPPS-TiO_2 could be produced at +0.2 V, at which the sensitizing effect of GSH could be observed, leading to the low-potential biosensing of GSH. The proposed photoelectrochemical biosensor showed good performance in the monitoring of GSH with a rapid response, wide concentration range, low applied potential, and good selectivity and could successfully be applied to the detection of reduced glutathione in gluthion injection (Scheme 1). The porphyrin-functionalized TiO_2 nanoparticles provide a robust approach for the photoelectrochemical detection of biomolecules.

Scheme 1. Schematic Illustration of Photoelectrochemical Process for Oxidation of GSH at FeTPPS-TiO_2-Modified ITO Electrode

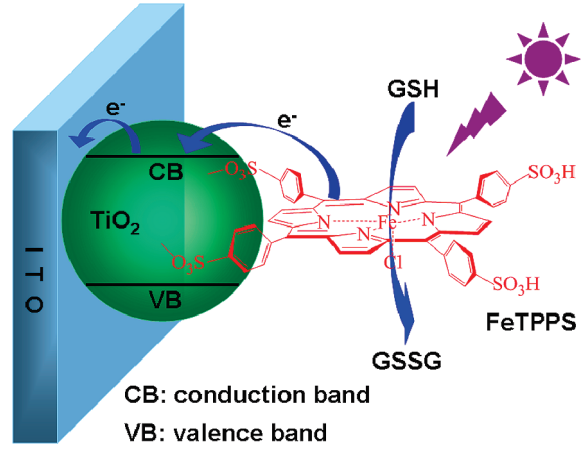

EXPERIMENTAL SECTION

Materials and Reagents. FeTPPS was a gift from Professor Osamu Ikeda at Kanazawa University (Kanazawa, Japan). TiO_2 nanopowder (anatase, <25 nm, 99.7%) and reduced L-glutathione (≥99%) were purchased from Sigma-Aldrich (St. Louis, MO). All other chemicals were of analytical grade. In this work, 0.1 mol L^{-1} phosphate buffer solution (PBS) was always employed as the supporting electrolyte after being deaerated with high-purity nitrogen. Reduced glutathione sodium for injection was produced by Pharminvest SPA (Milano, Italy). Aqueous solutions were prepared with twice-distilled water, and the pH value of PBS was 7.0 unless indicated otherwise.

Apparatus. Transmission electron microscopy (TEM) was performed using a JEM-2100 transmission electron microscope

(21) Tu, W. W.; Lei, J. P.; Ding, L.; Ju, H. X. *Chem. Commun.* **2009**, 4227–4229.
(22) Franco, R.; Panayiotidis, M. I.; Cidlowski, J. A. *J. Biol. Chem.* **2007**, *282*, 30452–30465.
(23) Wu, G. Y.; Fang, Y.-Z.; Yang, S.; Lupton, J. R.; Turner, N. D. *J. Nutr.* **2004**, *134*, 489–492.
(24) Roederer, M.; Staal, F. J.; Anderson, M.; Rabin, R.; Raju, P. A.; Herzenberg, L. A.; Herzenberg, L. A. *Ann. N.Y. Acad. Sci.* **1993**, *667*, 113–125.
(25) Bains, J. S.; Shaw, C. A. *Brain Res. Rev.* **1997**, *25*, 335–358.
(26) Chen, Z. Z.; Li, Q. L.; Wang, X.; Wang, Z. Y.; Zhang, R. R.; Yin, M.; Yin, L. L.; Xu, K. H.; Tang, B. *Anal. Chem.* **2010**, *82*, 2006–2012.
(27) Wang, Y.; Lu, J.; Tang, L. H.; Chang, H. X.; Li, J. H. *Anal. Chem.* **2009**, *81*, 9710–9715.
(28) Sudeep, P. K.; Joseph, S. T. S.; Thomas, K. G. *J. Am. Chem. Soc.* **2005**, *127*, 6516–6517.
(29) Ahn, Y.-H.; Lee, J.-S.; Chang, Y.-T. *J. Am. Chem. Soc.* **2007**, *129*, 4510–4511.
(30) Zhang, Y.; Li, Y.; Yan, X.-P. *Anal. Chem.* **2009**, *81*, 5001–5007.
(31) Yao, Z. Y.; Feng, X. L.; Li, C.; Shi, G. Q. *Chem. Commun.* **2009**, 5886–5888.
(32) Liu, J. F.; Bao, C. Y.; Zhong, X. H.; Zhao, C. C.; Zhu, L. Y. *Chem. Commun.* **2010**, 2971–2973.
(33) Raththagala, M.; Root, P. D.; Spence, D. M. *Anal. Chem.* **2006**, *78*, 8556–8560.
(34) Huang, G. G.; Han, X. X.; Hossain, M. K.; Ozaki, Y. *Anal. Chem.* **2009**, *81*, 5881–5888.
(35) Huang, Y.-F.; Chang, H.-T. *Anal. Chem.* **2007**, *79*, 4852–4859.
(36) Safavi, A.; Maleki, N.; Farjami, E.; Mahyari, F. A. *Anal. Chem.* **2009**, *81*, 7538–7543.
(37) Pacsial-Ong, E. J.; McCarley, R. L.; Wang, W. H.; Strongin, R. M. *Anal. Chem.* **2006**, *78*, 7577–7581.
(38) Pournaghi-Azar, M. H.; Ahour, F. *J. Electroanal. Chem.* **2008**, *622*, 22–28.
(39) Kumar, S. M. S.; Pillai, K. C. *Electrochim. Acta* **2009**, *54*, 7374–7381.

(JEOL, Japan). Scanning electron microscopy (SEM) was performed using a Hitachi S-4800 scanning electron microscope (Hitachi, Tokyo, Japan). Resonance Raman spectra were recorded on a Renishaw-inVia Raman microscope (Renishaw, Gloucestershire, U.K.). X-ray photoelectron spectroscopy (XPS) measurements were performed using an ESCALAB 250 spectrometer (Thermo-VG Scientific, Waltham, MA) with ultrahigh vacuum generators. Ultraviolet−visible absorption spectra were recorded with a Lambda 35 UV/vis spectrometer (Perkin-Elmer Instruments, Wellesley, MA). Static water contact angles were measured with a contact angle meter (Ramé-Hart-100, Ramé-Hart, Netcong, NJ) using droplets of deionized water at 25 °C. Photoelectrochemical measurements were performed with a home-built photoelectrochemical system. A 500-W Xe lamp equipped with a monochromator was used as the irradiation source. Photocurrent was measured on a CHI 660D electrochemical workstation (CH Instruments, Austin, TX). All experiments were carried out at room temperature using a conventional three-electrode system with a modified indium tin oxide (ITO) electrode as the working electrode, a platinum wire as the auxiliary electrode, and a saturated calomel electrode as the reference electrode.

Preparation of FeTPPS-TiO_2 and Modified ITO Electrodes. TiO_2 (100 mg) was calcined in a muffle furnace at 450 °C for 30 min. After being allowed to cool to 50−80 °C, the calcined TiO_2 was added to 5 mL of FeTPPS solution (1.5 mg mL^{-1}). The suspension was sonicated for 30 min and kept at room temperature for 24 h. Then, the resulting suspension was centrifuged at 8000 rpm for 15 min to remove free FeTPPS. After being washed twice with twice-distilled water, the sediment was dried at 70 °C to obtain FeTPPS-TiO_2 nanoparticles.

After an ITO electrode had been cleaned with NaOH (1 mol L^{-1}) and H_2O_2 (30%), washed with acetone and twice-distilled water, and dried at room temperature, 10 μL of the FeTPPS-TiO_2 suspension (1 mg mL^{-1}) was coated onto the ITO electrode and dried at room temperature to obtain an FeTPPS-TiO_2-modified ITO electrode. A TiO_2-modified ITO electrode was prepared similarly.

RESULTS AND DISCUSSION

Characterization of FeTPPS-TiO_2. The morphologies of TiO_2 and FeTPPS-TiO_2 were observed by transmission electron microscopy. Compared with the aggregation of TiO_2 (Figure 1A), the TEM image of FeTPPS-TiO_2 in Figure 1B shows a more discernible and better dispersion, which is advantageous for the formation of a robust homogeneous film for the construction of a biosensor. The average diameter of the FeTPPS-TiO_2 nanoparticles was estimated to be 15 nm. The thickness of the FeTPPS-TiO_2 film on an ITO surface was estimated by SEM to be 0.85 μm (Figure 1C). The homogeneous film was beneficial for photoelectron transfer between FeTPPS-TiO_2 and the electrode.

The Raman spectrum of TiO_2 nanoparticles (Figure 2A, curve a) shows the characteristics of the anatase nanocrystalline structure at 393, 513, and 636 cm^{-1}, whereas that of FeTPPS (Figure 2A, curve b) does not show any obvious Raman peak between 300 and 740 cm^{-1}. After FeTPPS had been bonded to TiO_2, these characteristic bands of TiO_2 shifted slightly to 395, 514, and 638 cm^{-1} with strengths enhanced by 27.5%, 25.1%, and 33.0%, respectively (Figure 2A, curve c), which can be attributed to the charge-transfer mechanism of FeTPPS-TiO_2

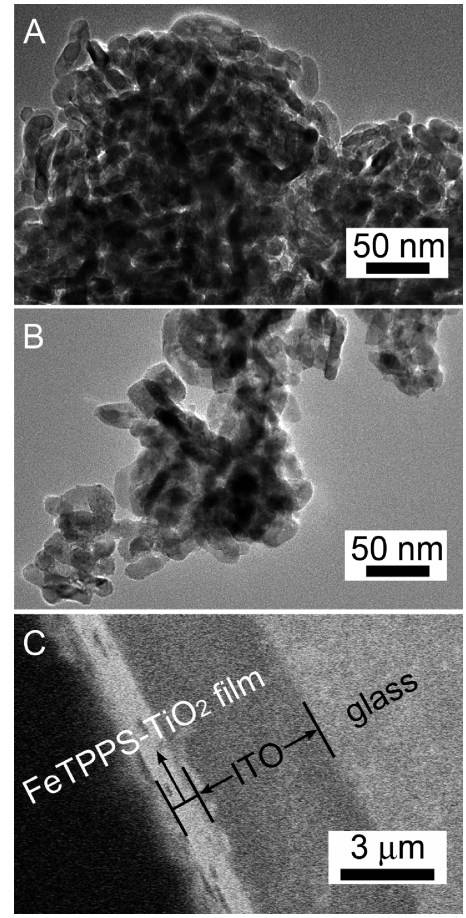

Figure 1. TEM images of (A) TiO_2 and (B) FeTPPS-TiO_2 nanoparticle suspensions at 1 mg mL^{-1} and (C) SEM section image of FeTPPS-TiO_2-modified ITO electrode.

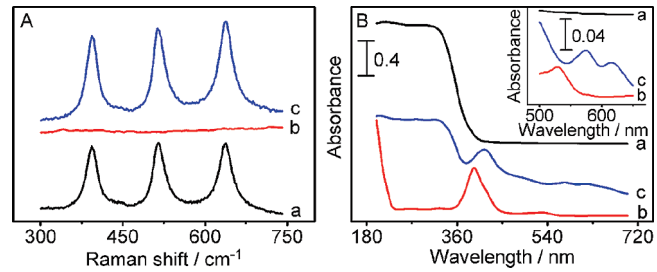

Figure 2. (A) Raman and (B) UV−vis absorption spectra of (a) TiO_2, (b) FeTPPS, and (c) FeTPPS-TiO_2 powders. Inset: amplified UV−vis absorption spectra.

related to the surface-state energy levels of the TiO_2 semiconductor.[40] In addition, no nanocrystalline structure of TiO_2 other than anatase was detected by Raman spectroscopic measurements.[41] This fact is of great importance for photocurrent generation in photovoltaic applications, because the anatase phase of TiO_2 has a larger surface area and faster electron transport than the rutile phase.[42] Moreover, after FeTPPS had been assembled on the surface of TiO_2, the TiO_2 anatase

(40) Yang, L. B.; Jiang, X.; Ruan, W. D.; Zhao, B.; Xu, W. Q.; Lombardi, J. R. *J. Phys. Chem. C* **2008**, *112*, 20095–20098.
(41) Imahori, H.; Hayashi, S.; Umeyama, T.; Eu, S.; Oguro, A.; Kang, S.; Matano, Y.; Shishido, T.; Ngamsinlapasathian, S.; Yoshikawa, S. *Langmuir* **2006**, *22*, 11405–11411.
(42) Park, N.-G.; Lagemaat, J.; Frank, A. J. *J. Phys. Chem. B* **2000**, *104*, 8989–8994.

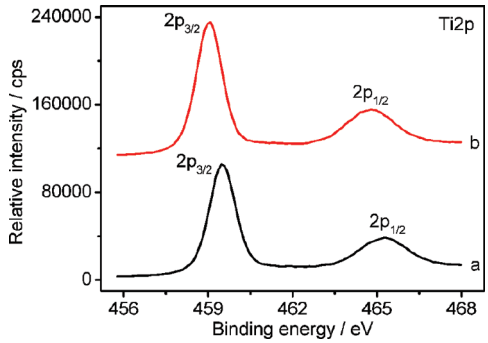

Figure 3. Ti 2p XP spectra of (a) TiO_2 and (b) FeTPPS-TiO_2 powders.

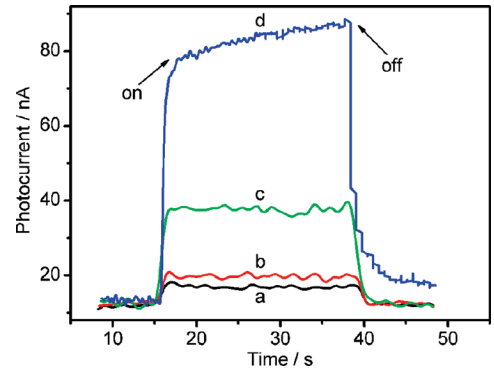

Figure 4. Photocurrent responses of (a,b) TiO_2- and (c,d) FeTPPS-TiO_2-modified ITO electrodes in 0.1 M pH 7.0 PBS in the (a,c) absence and (b,d) presence of 800 μmol L^{-1} GSH at +0.2 V to a light excitation at 380 nm.

nanocrystalline structure retained the three characteristics bands, indicating that the functionalization of TiO_2 nanoparticles with FeTPPS did not damage the conjugation of the TiO_2 nanoparticles.[41]

The UV−vis absorption spectra of TiO_2, FeTPPS, and FeTPPS-TiO_2 are shown in Figure 2B. TiO_2 did not show any UV−vis absorption above 400 nm (curve a), whereas FeTPPS exhibited a typical Soret band absorption at 392 nm and a weak Q-band absorption at 529 nm (curve b). In the presence of TiO_2, the Soret band of FeTPPS-TiO_2 showed a decrease of intensity with a red shift from 392 to 415 nm, and the Q-band of FeTPPS-TiO_2 split into two adsorption peaks at 575 and 617 nm (curve c), which can be attributed to the dentate binding of TiO_2 with sulfonic groups of FeTPPS. Otherwise, no obvious change of the absorption spectrum could be observed, as reported for the physical absorption of meso-tetrakis(4-phenyl)porphyrin on TiO_2 nanoparticles in a previous work.[15]

The XP spectrum of Ti 2p was recorded to further characterize the formation of FeTPPS-TiO_2 nanoparticles (Figure 3). The Ti 2p XP spectrum of TiO_2 consisted of two peaks assigned to Ti $2p_{1/2}$ at 465.32 eV and Ti $2p_{3/2}$ at 459.49 eV (curve a). Compared with these peaks, the Ti $2p_{1/2}$ and Ti $2p_{3/2}$ peaks of FeTPPS-TiO_2 shifted to lower binding energies of 464.75 and 459.04 eV, respectively (curve b). These changes were attributed to the coordination of Ti atom as the acceptor by oxygen atom in FeTPPS-TiO_2 as an electron donor,[43] confirming the dentate binding of TiO_2 nanoparticles with the sulfonic groups of FeTPPS.

The biocompatibility of the novel functional TiO_2 nanoparticles was characterized by contact angle measurements. The contact angles of a bare glass slide and TiO_2 and FeTPPS-TiO_2 films were measured to be 32.3°, 21.0°, and 6.8°, respectively. The smallest contact angle of the FeTPPS-TiO_2 film indicates the best hydrophilicity, which is attributed to more hydrophilic groups introduced by water-soluble FeTPPS. The good biocompatibility of FeTPPS-TiO_2 could greatly improve the bioactivity of immobilized FeTPPS for photoelectrochemical biosensing.

Photoelectrochemical Oxidation of GSH. Upon photoexcitation at a wavelength of 380 nm, the TiO_2-modified ITO electrode showed a photocurrent of 5.6 nA at an applied potential of +0.2 V (Figure 4, curve a), whereas the FeTPPS-TiO_2-modified ITO electrode showed a photocurrent of 25.2 nA (Figure 4, curve c), indicating the improvement of the photo-current conversion efficiency of TiO_2 by the addition of FeTPPS because of the strong electronic coupling between the excited-state FeTPPS and the conduction band of TiO_2. Furthermore, the improved photo-current conversion efficiency could be further amplified by an electron-transfer process from other biomolecules to FeTPPS. Using GSH as a model, upon addition of 800 μmol L^{-1} GSH, the photocurrent of FeTPPS-TiO_2-modified ITO electrode increased by 50.1 nA (Figure 4, curves c and d), which was 17.3 times the photocurrent increment of 2.9 nA observed at the TiO_2-modified ITO electrode (Figure 4, curves a and b). The increase of 52% at the TiO_2-modified ITO electrode is attributed to the oxidization of GSH by the TiO_2 holes.[8] The different sensitizing effect at FeTPPS-TiO_2-modified ITO electrode with an increase of 199% resulted from the efficient charge separation of the FeTPPS-TiO_2 system to form electron−hole pairs for the photoelectrochemical oxidation of GSH.

The photoelectrochemical process of FeTPPS-TiO_2 for the GSH oxidation is proposed in Scheme 1. The oxidation potential of the excited state of FeTPPS is −0.82 V,[44] which is lower than the −0.1 V of the conduction band energy level of TiO_2.[15] Thus, the electron transfer from the excited state of FeTPPS to the conduction band of TiO_2 is thermodynamically favorable for generating electron−hole pairs under irradiation. In the presence of GSH, GSH as an electron donor and sacrificial reagent can transfer electrons to the holes located on the excited state of FeTPPS, and these electrons can then quickly inject into the conduction band of the TiO_2 nanoparticles. Finally, photoexcitation electrons transfer to the ITO electrode, leading to a sharp increase of the photocurrent. During this process, GSH was oxidized to glutathione disulfide (GSSG). Moreover, the current was relatively stable over time and could be turned on and off by controlling the light.

Condition Optimization. As shown in Figure 5A, upon addition of 800 μmol L^{-1} GSH, the photocurrent increment decreased at the applied potential of +0.2 V as the exciting wavelength increased from 350 to 400 nm. The photocurrent increment at 380 nm was 62% of that at 350 nm, showing enough sensitivity for photoelectrochemical detection of GSH.

(43) Li, D.; Dong, W. J.; Sun, S. M.; Shi, Z.; Feng, S. H. *J. Phys. Chem. C* **2008**, *112*, 14878–14882.

(44) Kalyanasundaram, K.; Neumann-Spallart, M. *J. Phys. Chem.* **1982**, *86*, 5163–5169.

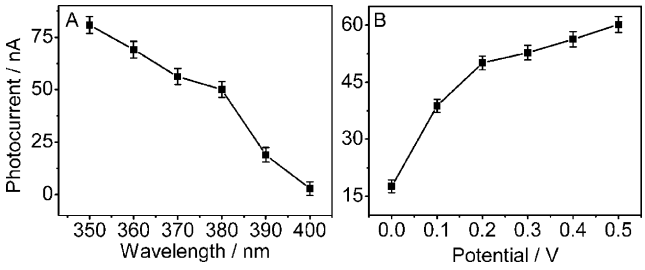

Figure 5. Effects of (A) excitation wavelength and (B) applied potential on photocurrent response of FeTPPS-TiO_2-modified ITO electrode in 0.1 M pH 7.0 PBS containing 800 μmol L^{-1} GSH.

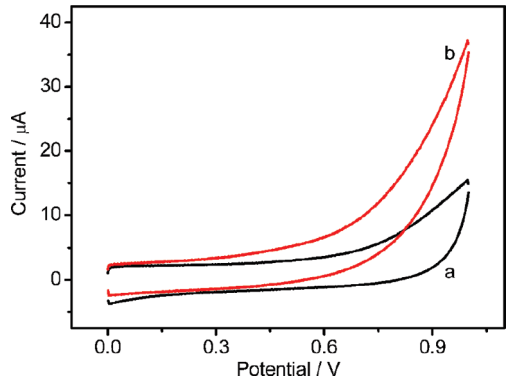

Figure 6. Cyclic voltammograms obtained at FeTPPS-TiO_2-modified ITO electrode in 0.1 M pH 7.0 PBS in the (a) absence and (b) presence of 800 μmol L^{-1} GSH at 100 mV s^{-1}.

Afterward, the photocurrent increment quickly decreased. Furthermore, a long wavelength means low energy consumption, which is favorable for the monitoring of biological systems. Thus, 380 nm was chosen for the photoelectrochemical biosensing of GSH.

The applied potential is an important parameter for producing the photocurrent. Upon addition of 800 μmol L^{-1} GSH, the photocurrent increment sharply increased as the applied potential increased from 0 to +0.2 V and then trended toward a maximum value (Figure 5B). The photocurrent increment at +0.2 V was 83% of that at +0.5 V, showing sufficient sensitivity for the photoelectrochemical detection of GSH. To exclude the interference of other reductive species coexisting in the samples, +0.2 V was chosen for the photoelectrochemical biosensing of GSH.

The photocurrent of the FeTPPS-TiO_2-modified ITO electrode depends on the concentration of GSH, giving rise to a method for the detection of GSH at the applied potential of +0.2 V. Notably, this potential is much lower than that used for the amperometric detection of GSH. As shown in Figure 6, the cyclic voltammogram of the FeTPPS-TiO_2-modified ITO electrode did not show any observable peak in the potential range from 0 to +1.0 V. After 800 μmol L^{-1} GSH had been added to PBS, although the electrochemical oxidation of GSH at the FeTPPS-TiO_2-modified ITO electrode started at +0.2 V, the slow electron-transfer rate in the oxidation process of GSH led to a high overpotential; thus, no obvious oxidation peak could be observed until the potential was scanned to +1.0 V. The obvious increase of anodic current occurred at potentials more positive than +0.75 V. However, the sensitivity for amperometric detection of GSH at an applied potential of +0.75 V was much

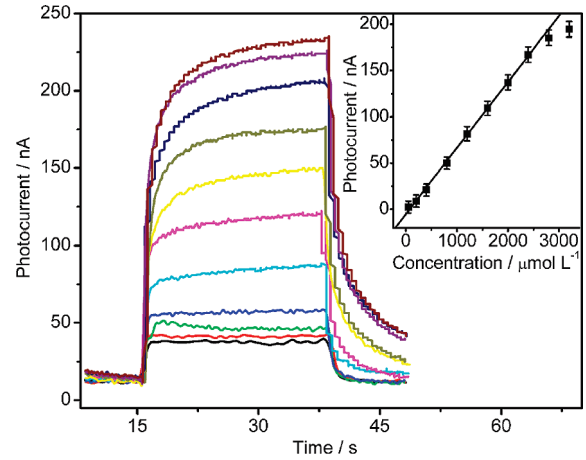

Figure 7. Photocurrent responses at FeTPPS-TiO_2-modified ITO electrode in 0.1 M pH 7.0 PBS in the presence of 0, 50, 200, 400, 800, 1200, 1600, 2000, 2400, 2800, and 3200 μmol L^{-1} GSH (from bottom to top) at +0.2 V to a light excitation at 380 nm. Inset: linear calibration curve.

higher than that for photoelectrochemical detection under 380-nm irradiation at +0.2 V, showing an advantage of the photoelectrochemical detection in terms of applied potential. As mentioned above, the low applied potential is favorable for the elimination of interference from other reductive species coexisting in the samples.

Photoelectrochemical Detection of GSH. The photocurrent−time curve of FeTPPS-TiO_2-modified ITO electrode clearly illustrates the rapid response of the modified electrode to GSH at an applied potential of +0.2 V (Figure 7). Under the optimal conditions, the response displayed a linear increase as the GSH concentration increased from 0.05 to 2.4 mmol L^{-1} with a detection limit of 0.03 mmol L^{-1}. The linear response range was wider than those of the electrogenerated chemiluminescence of quantum dots (0.024−0.214 mmol L^{-1}),[27] the fluorometric method (0.025−0.25 mmol L^{-1}),[31] and surface-enhanced Raman scattering (0.1−0.8 μmol L^{-1}).[34] Although the detection limit of 30 μmol L^{-1} was higher than the 8.3 μmol L^{-1} of the previous method,[27] the upper limit of detection (2.4 mmol L^{-1}) is more suitable for the photoelectrochemical detection of GSH in biological samples because the normal level of GSH in human fluids is in the range of 0.1−10 mmol L^{-1}.[24] The response could reach the steady signal within only 15 s. Thus, the time for the detection of GSH was much shorter than the 5 min for the Raman scattering sensing method[34] and 50 s for microchip electrophoresis-laser induced fluorescence.[26] Obviously, the proposed FeTPPS-TiO_2-based photoelectrochemical biosensor shows promise for application in the monitoring of GSH with a wide concentration range and short detection time.

Stability of FeTPPS-TiO_2-Based Biosensor. The photoelectrochemical biosensor for GSH showed good fabrication reproducibility with a relative standard deviation of 5.6% estimated from the slopes of the calibration plots of five freshly prepared FeTPPS-TiO_2-modified ITO electrodes. At GSH concentrations of 400 and 1600 μmol L^{-1}, the photoelectrochemical biosensor showed good repeatability with relative standard deviations of 5.8% and 5.3%, respectively, examined for five determinations.

When the photoelectrochemical biosensor was not in use, it was stored in the shade at room temperature and measured every

few days. No obvious decrease in the photocurrent response to GSH was observed after 10 days, and 94.6% of the initial photocurrent response was maintained after 4 weeks. This implies that the structure of FeTPPS-TiO_2 is efficient for retaining the activity of FeTPPS and preventing it from leaking out of the photoelectrochemical biosensor.

Interference and Application in Real-Life Samples. Because GSH is the auxiliary for the chemotherapy of cancer, the effects of anticancer drugs as interfering species on the photoelectrochemical biosensing response were examined. For example, cisplatin, fluorouracil, and adriamycin at 10 times the concentration of GSH did not interfere with the photoelectrochemical response of GSH. Thus, the photoelectrochemical biosensor had an excellent specificity for the detection of GSH in samples with anticancer drugs.

The concentration of reduced glutathione in gluthion injection was detected with the proposed photoelectrochemical biosensor to be 0.018 ± 0.002 mol L^{-1} (five measurements) without any need of sample pretreatment except for appropriate dilution. This value was consistent with the 0.017 mol L^{-1} value given in the instruction on glutathione injection, indicating acceptable accuracy of the photoelectrochemical biosensor.

CONCLUSIONS

A novel photoelectrochemical biosensing platform was developed using newly synthesized FeTPPS-TiO_2 nanoparticles, which were prepared by the dentate binding of TiO_2 nanoparticles with sulfonic groups of FeTPPS and exhibited good biocompatibility and dispersion in water. FeTPPS could efficiently improve the photo-current conversion efficiency of the TiO_2 nanoparticles, which could be further amplified by an electron-transfer process from biomolecules to FeTPPS. Using GSH as a model, the fast photoelectronic communication among GSH, FeTPPS, TiO_2, and ITO electrode led to a novel method for the photoelectrochemical detection of GSH with good analytical performance, such as low applied potential, rapid response, wide linear range, and good reproducibility and repeatability. The low-potential detection produced excellent specificity for excluding the interference of other reductive species and anticancer drugs in real samples. Taking into account that iron porphyrin can mimic peroxidase, this approach could be used for hydrogen peroxide detection. The proposed photoelectrochemical biosensor showed promising application in the monitoring of biomolecules that could donate electrons to hole-injected FeTPPS. These porphyrin-functionalized TiO_2 nanoparticles open a new avenue for the construction of photoelectrochemical biosensors.

ACKNOWLEDGMENT

This work was financially supported by the National Basic Research Program of China (2010CB732400); the National Science Funds for Creative Research Groups (20821063); the Major Research Plan (90713015), Key (20835006), and General Programs (20875044, 20705012, 21075060) from the National Natural Science Foundation of China; and the Ph.D. Fund for Young Teachers (20070284052).

Received for review August 5, 2010. Accepted September 10, 2010.

AC102070F